Exp. Theo. NANOTECHNOLOGY 10 (2026) 795-809 https://doi.org/10.56053/10.2.795

Fabrication and characterization of titanium dioxide thin films with various temperatures fabrication via sol-gel technique

Abdul Rasool J. Katae[1], Hassan Hadi Hussein[1], Ahmed Shawki Jaber[2], Mohammed Abdulhadi Sarhan[2], Mohammed RASHEED[3,]*

[1]Applied Sciences Department, University of Technology- Iraq, Baghdad 10066, Iraq
[2]Mathematics Science Department, College of Science, Mustansiriyah University, Baghdad, Iraq
[3]College of Production Engineering & Metallurgy, University of Technology- Iraq, Baghdad, Iraq
[*]) Email: rasheed.mohammed40@yahoo.com

Received 11/1/2026, *Received in revised form* 13/3/2026, *Accepted* 30/3/2026, *Published* 15/4/2026

Titanium dioxide films TiO_2 have been deposited by dip-coating technique with different temperatures 300, 350, and 400 °C. The objective of this work is to study of the characterization of TiO_2 thin films under different temperatures. The films are synthesized by dip-coating technique and examined by X-ray diffraction (XRD). Hall effect is performed to measure the electrical properties of the samples. The results obtained by XRD confirm the formation of TiO_2 films with a tetragonal structure and crystallite size varies from (15.0 – 5.1) nm. Deposited films with resistivity vary of (130 to 60) Ω.cm, figure of merite F_{TC} varies from (1.78×10^{-8} to 3.93×10^{-8}) $(\Omega/sq)^{-1}$ respectively. Optical band gap and urbach energy (3.35 – 3.22 and 0.42 – 0.37) eV, all the values at 550 nm have been obtained.

Keywords: Optical; TiO_2; Sol-gel; Electrical.

1. INTRODUCTION

Titanium dioxide is a chemically inert, biocompatible crystaline inorganic solid that is optically transparent and such properties have made it versatile material for applications [1-3]. Being characterized by a high refractive index and good UV absorbing and photo-activity properties, it is widely used in a wide range of fields such as: photocatalysis [4,5], paints and coatings [6], photovoltaics [7], catalysis [8], optical devices [9]and biomedical applications [10]. TiO_2-nanoparticles used in medical area are widely applied on drug carriers, imaging and photodynamic therapy [11]. This is only a hint for the role of TiO_2 [12]. The broad acceptance is an indication of its applicational flexibility and ease of integration in many fields which becomes attractive research and technology topic for academic research labs as well as industry [13]. More features (like synthesis strategies,

applications) about TiO_2 as a kind of the research by-products and their scientific and technical frontiers will also be explored in [14]. Since conventional dip-coating is a frequently used process of thin-film deposition in material science and semiconductor technology, not only to control the film thickness accurately but also ensure uniformity [15,16], we describe the case of the film formation process by this method below. Titanium dioxide (TiO_2) is one of the popular materials for dotting process, which is commonly used in solar cell, optical films and micro-electronics industries [17-20]. Glass is used as a substrate and the dip-coating technique to deposit thin TiO_2 layers in our work. The deposits are grown in ambient and annealed for 2 hours at 300,350 and 400 oC. From UV-visible absorption spectroscopy, the energy of the optical band gap and transmittance are calculated. The TiO_2 layer produced in this manner is characterised using X-ray diffraction (XRD), optical transmission spectrophotometry (UV-vis) and FTIR spectroscopy as complementary experimental means of study. The thickness of the samples has been calculated using gravimetric method.

2. EXPEREMINTAL PART

Titanium diode thin films are prepared via dip-coating technique, titanium isopropoxide, TTIP-$Ti\{OCH(CH_3)_2\}_4$, (99.99%, MW=284.2153 g/mol)as a precursor sources, is dissolved in a mixtures of ethanolCH_3CH_2OH(EtOH, Biochem- 99%,MW= 46.07g/mol),Hydrochloric acid, HCL (37%; MW=36.46 $g.mol^{-1}$), and deionized water H_2O(conductivity (20 ^oC)≤ 4.3 uS/cm, MW= 18.02 g/mol) to create a sol-gel of TiO_2 are purchased from sigma-Aldrich, USA. TTIP is held at a constant concentration of 0.5 M using a magnetic stirrer; the liquid is agitated at 80 °C for 3 hours to produce a clear and viscous solution. The sols are then left at room temperature under cover for 24 hours before being put on the substrates. Under ambient conditions, the thin films are produced using the dip coating process at withdrawal speeds of 100 mm/min. All samples are heated to 200 °C for 15 minutes after each deposition to evaporate the solvent. Finally, the films are annealed at 300, 350, and 400 °C for 2 hours.

UV-Vis-NIR spectrophotometer type JASCO V630 DUO/5G; double-beam recording spectrophotometer with a spectral range from 200 to 1100 nm has been used for optical properties of films. The crystallitography parameters has been identified by X-ray diffraction (XRD) analysis using a (ARL EQUINOX 100) X-ray, 40 kV, 0.9 mA, CuKα 1,2 (λ=0.154056 nm) radiation in a wide range of Bragg angles ($0 \leq 2\theta \leq 90$) at a scanning rate of 2^o min^{-1}.

3. RESULT AND DISCUSSION

3.1. Thickness measurements

The thickness (t) of TiO_2 based thin films is estimated by the gravimetric method using the relation [16, 21-23]

$$t = M/\rho.A \quad (1)$$

where t is the films thickness (cm), A is the surface area of the films (cm^2), $M$is the mass of the films (g), and ρ is the density of the film material ($g.cm^3$). Thicknesses of TiO_2 films using gravimetric method is t_1=222±0.03 nm, t_2=200±0.01 nm, and t_3=190±0.04 nm for TiO_2 films at 300, 350, and 400 ^oC, respectively.

3.2. Optical properties

Figure 1 presents the transmission spectra of TiO_2 films with different temperatures 300, 350 and 400 ^oC with against wavelength (λ). The increasing transmission of TiO_2 thin films with higher temperatures suggests improved optical quality and reduced scattering or absorption of light at a

wavelength of 600 nm. This behavior can be advantageous in various optical and optoelectronic applications where controlling the transparency of thin films is essential for achieving desired performance characteristics. The trend of increasing transmission with increasing temperature indicates that as the temperature during film deposition or annealing increases, the TiO_2 thin films become more transparent to light at the given wavelength of 600 nm [24, 25].

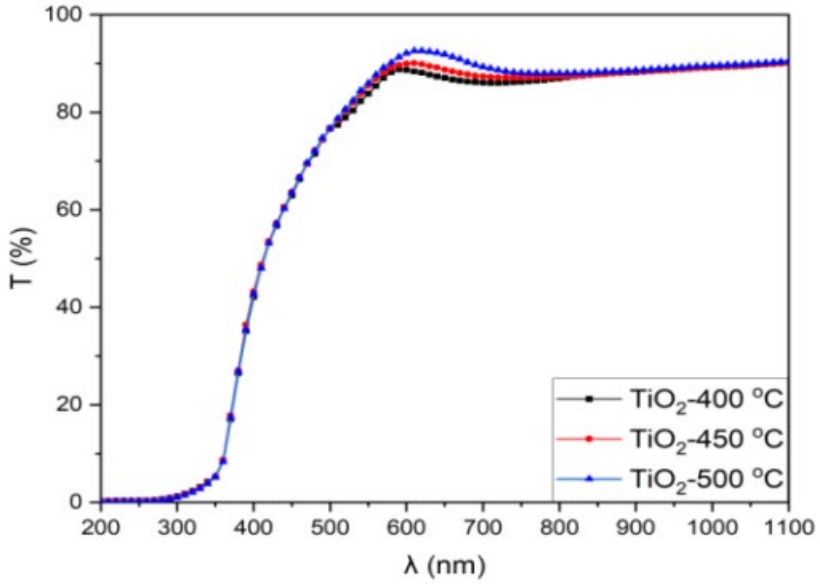

Figure 1 Transmission spectra of $TiO_2$with 300, 350 and 400 ^oC.

The reflection values in the visible region (VIS) show a clear trend of decreasing reflection with increasing temperature. Specifically, as the temperature increases from 300°C to 400°C, the reflection decreases from 9.9% to 7.4% as shown in Figure 2. The reflection spectra of TiO_2 thin films at different temperatures show a clear decrease in reflection in the visible region with increasing temperature, while the reflection in the NIR region remains relatively stable. These observations provide valuable insights into the optical properties of the films and their potential applications in both visible and NIR optical systems. The decreasing reflection in the visible range indicates that TiO_2 thin films become more optically transparent at higher temperatures within the visible spectrum [17,26-30].

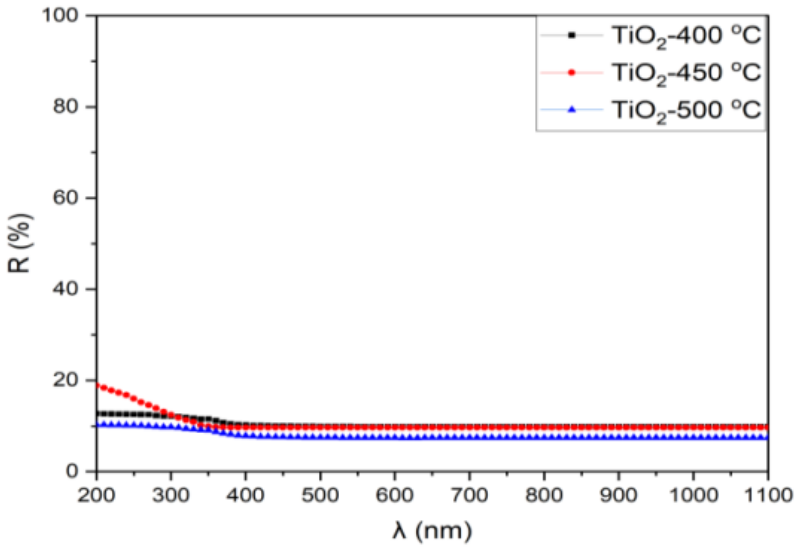

Figure 2 Reflection spectra of TiO_2 with 300, 350 and 400 °C.

The absorption values in the visible region show a notable trend of variation with temperature. As the temperature increases from 300°C to 400°C, the absorption values change as follows: 12.8, 12.08, and 13.16 as shown in Figure 3. The increase in absorption with increasing temperature suggests that TiO_2 thin films become more absorptive in the visible region at higher temperatures. The absorption values can be associated with the ability of the films to absorb and convert incoming photons into electronic excitations. The increase in absorption at higher temperatures could be related to changes in the film's electronic structure or bandgap [18, 31-35].

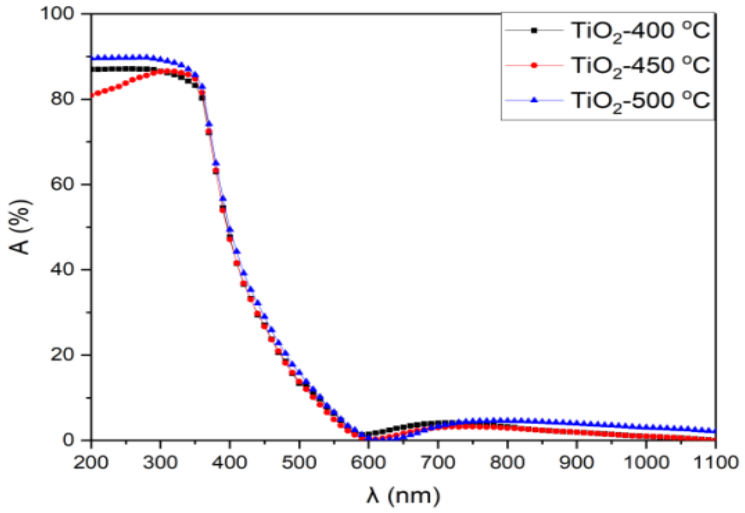

Figure 3 Absorption spectra of TiO_2films with 300, 350 and 400 °C.

As the temperature increases from 300°C to 400°C, the absorption coefficient values change as follows: 5332.3, 4722.4, and 4057.2cm^{-1}as shown in Figure 4. The decrease in absorption coefficient with increasing temperature suggests that TiO_2 thin films become less absorptive in the visible region

at higher temperatures. This behaviour is consistent with the idea that as the temperature increases, the films become more transparent to visible light [19, 36-40].

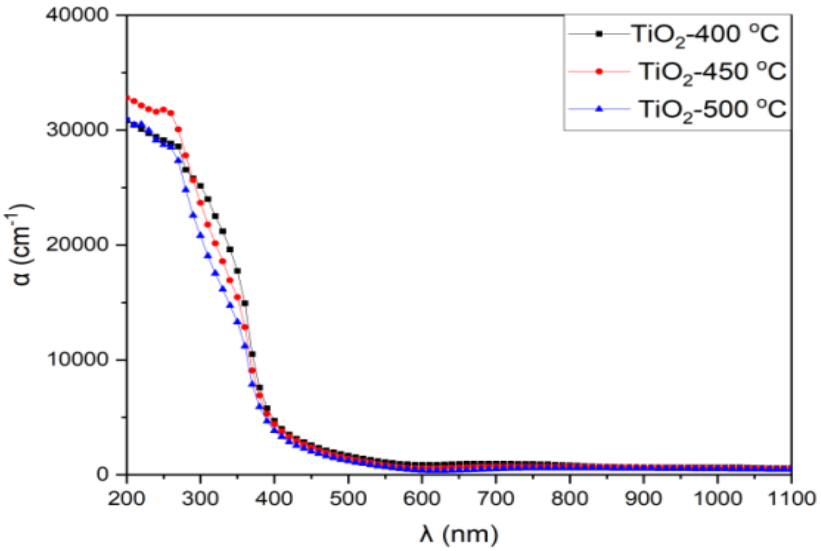

Figure 4 Absorption coefficient spectra of TiO_2 with 300, 350 and 400 °C.

The extinction coefficient values in the visible region show a trend of decreasing values with increasing temperature. Specifically, as the temperature increases from 300°C to 400°C, the extinction coefficient values change as follows: 0.0066, 0.005, and 0.004 as shown in Figure 5.The reported extinction coefficient values in the visible range are relatively low (in the order of 0.004 to 0.0066). This indicates that TiO_2 thin films are generally transparent or have weak absorption in the visible part of the electromagnetic spectrum [20, 41, 42].

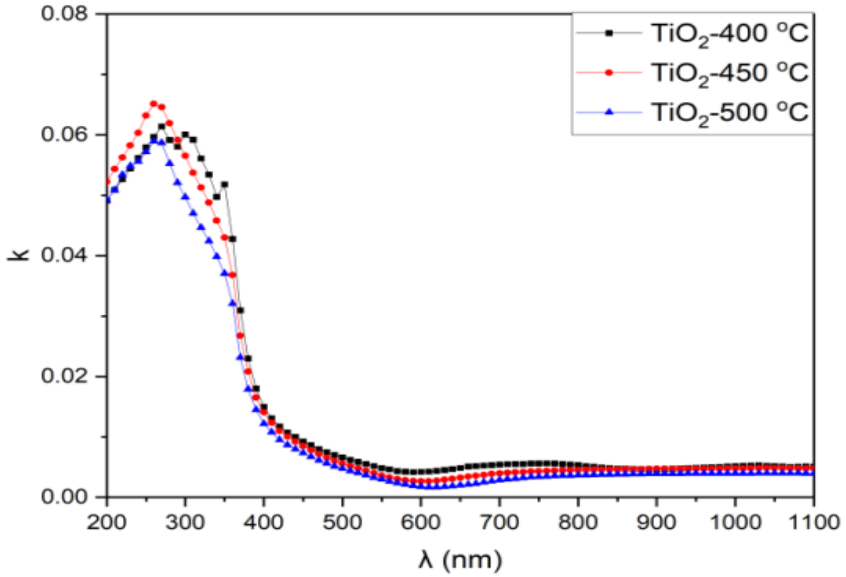

Figure 5 Extinction coefficient spectra of TiO_2 with 300, 350 and 400 °C.

Specifically, as the temperature increases from 300°C to 400°C, the refractive index values change as follows: 2.06, 1.91, and 1.75 as shown in Figure 6. The decrease in refractive index with increasing temperature suggests that TiO_2 thin films become optically less dense and exhibit weaker optical dispersion in the visible region at higher temperatures. This behaviour indicates that as the temperature increases, the films become more transparent to visible light and have reduced light-bending capabilities [21,43,44].

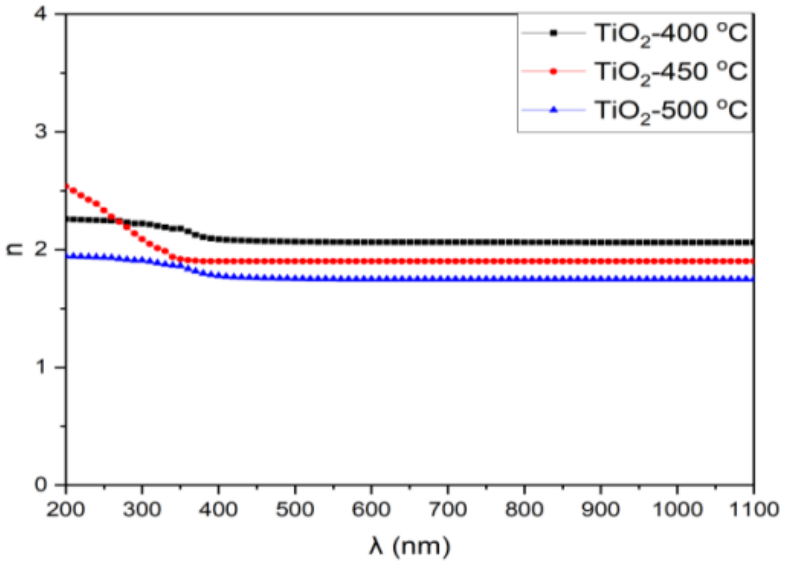

Figure 6 Refractive index spectra of TiO_2 with 300, 350 and 400 °C.

The real dielectric constant values in the visible region exhibit a clear trend of decreasing values with increasing temperature. Specifically, as the temperature increases from 300°C to 400°C, the real dielectric constant values change as follows: 4.27, 3.61, and 3.07 as shown in Figure 7. The decrease in the real dielectric constant with increasing temperature suggests that TiO_2 thin films become less polarizable and exhibit weaker dielectric response to electric fields in the visible region at higher temperatures. This behaviour indicates that as the temperature increases, the films become less effective at storing electrical energy when subjected to electromagnetic fields in the visible range [22,45,46].

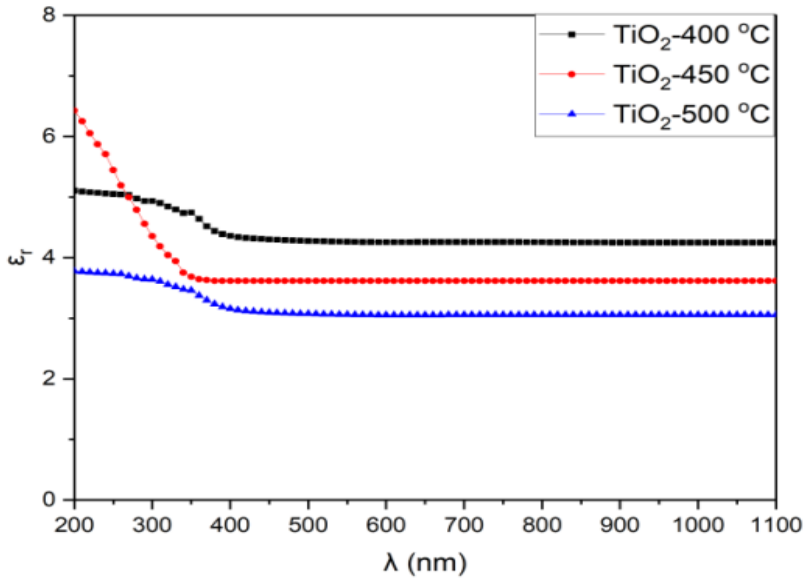

Figure 7 Real part of dielectric constant spectra of TiO_2 with 300, 350 and 400 °C.

The imaginary dielectric constant values in the visible region show a clear trend of decreasing values with increasing temperature. Specifically, as the temperature increases from 300°C to 400°C, the imaginary dielectric constant values change as follows: 0.027, 0.02, and 0.015 as shown in Figure 8. The decrease in the imaginary dielectric constant with increasing temperature suggests that TiO_2 thin films become less absorptive or exhibit weaker absorption of electromagnetic energy in the visible region at higher temperatures. This behaviour indicates that as the temperature increases, the films become more transparent or less absorbing to electromagnetic radiation in the visible part of the spectrum [47].

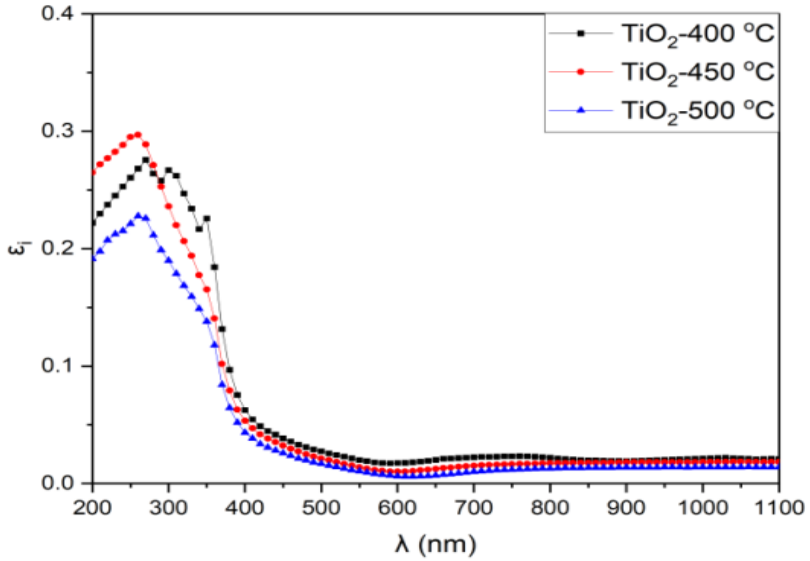

Figure 8 Imaginary part of dielectric constant spectra of TiO_2 with 300, 350 and 400 °C.

The optical band gap energy is determined utilizing the Tauc plot equation as follows [23,24]

$$(\alpha h\nu)^n = A(h\nu - E_g) \quad (2)$$

E_g can be obtained in the extrapolation of the linear segment of the $(\alpha h\upsilon)^2$ versus $h\nu$ plot intercepts the energy axis at($\alpha h\upsilon = 0$), as illustrated in Figure 9. This figure presents the optical energy gap (or indirect bandgap) of TiO_2(n-type semiconductor) thin films at different temperatures (300 , 350 , and 400 °C) with values of 3.35 , 3.26 , and 3.22 eV, respectively, provides insights into how the bandgap changes with temperature. The trend of decreasing bandgap with increasing temperature suggests that the TiO_2 thin films become less insulating and more semiconducting as the temperature rises. A smaller bandgap indicates that less energy is required to promote electrons from the valence band to the conduction band [45].

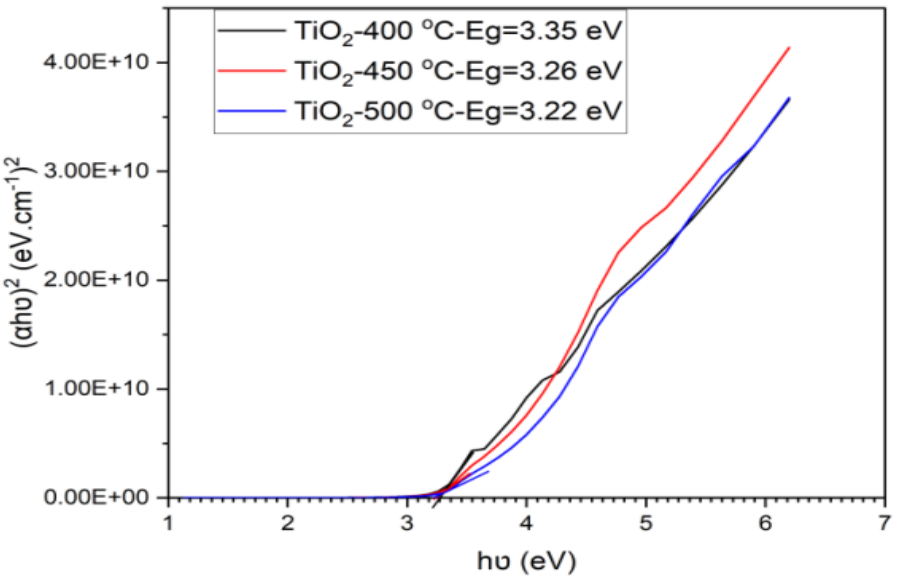

Figure 9 Optical energy of TiO_2 with 300, 350 and 400 °C.

The Urbach energy of the samples TiO_2-300 °C, TiO_2-350 °C, TiO_2-400 °C with their thicknesses 222, 200 and 190 nm, respectively is 0.42022, 0.40045 and 0.37582 eV, respectively has been calculated using the following equation [25, 26]

$$ln\alpha = ln\alpha_o + \frac{h\upsilon}{E_u} \quad (3)$$

where α is absorption coefficient. Therefore, the band tail energy or Urbach energy (E_u) can be obtained from the slope of the straight line of plotting $ln\alpha$ against the incident photon energy ($h\upsilon$) (not shown here). The decrease in Urbach energy with a decrease in the energy gap (Eg) of TiO_2 thin films at higher temperatures is generally associated with improvements in the material's crystalline quality, reduced disorder, and more well-defined electronic band structure.

3.3. X-ray diffraction

XRD pattern of synthesized TiO_2 nanostructures by sol-gel reaction at (300, 350 and 400) °C is shown in Figure10. All peaks of the obtained product are corresponding to the tetragonal structure of TiO_2 [27]. The crystal structure is observed between 0 to 90° diffraction angles. Figure 4 revealed the diffraction angles (2θ values) of planes (110), (004), (200), and (105) are 24.9967°, 37.7503°, 48.00302°, and 53.89236° respectively. For all the samples four main peaks appeared at (101), (004), (200), and (105) planes revealed that the TiO_2 films had polycrystalline nature, [α, γ, β= 90°], anatase phase with space group 141/a m d:1 (141). These peaks are in accordance with JCPDS data code no. (00-900-8213) for TiO_2 at 300, 350, and 400 °C, respectively. Furthermore, the average crystal size (D) is calculated for all samples by Scherrer's formula given in the following equation [28]:

$$D = \frac{k\lambda}{\beta cos\theta} \tag{4}$$

where k is the constant and its value is 0.9, λ is the X-ray wavelength, β and θ are the full wdth maximum (FWHM) and Bragg's angle of preferred diffraction peak respectively. The lattice strain and dislocation density of TiO_2 films are calculated by the following formulas [29-31]:

$$\varepsilon = \frac{\beta}{4tan\theta} \tag{5}$$

$$\delta = \frac{1}{D^2} \tag{6}$$

Similarity lattice constants are calculated by the following formulas [32-35]:

$$a = \frac{\lambda}{\sqrt{3}sin\theta} \tag{7}$$

$$c = \frac{\lambda}{sin\theta} \tag{8}$$

The integral breadth for each peak is determined using the following equation [36-40]:

$$\text{Integral Breadth= Area under the peak/Height of peak} \tag{9}$$

The comparison of grain size, lattice constants, inter-planer distance, lattice strain, dislocation density, among TiO_2 films using different temperatures (300, 350, and 400) °C and the comparison of all the above values showed in Table 1.

Table 1 Comparison of inter-planer distance, grain size, lattice strain, dislocation density, FWHM, and Integral Breadth.

TiO_2	2θ (°)	hkl	β (FWHM)	d(A°)	D (nm)	ε (m)	δ (m)	Integral Breadth
TiO_2-300 °C	24.9967	101	0.31466	0.35594227	25.86004114	1.340E-12	1.49E-12	0.334944134
	37.7503	004	1.5185	0.23810918	5.528985783	6.269E-12	3.271E-11	1.616396255
	48.00302	200	0.15061	0.189374235	57.73991768	6.003E-13	2.999E-13	0.160321856
	53.89236	105	0.06163	0.169986608	144.6020216	2.397E-13	4.783E-14	0.06559899
TiO_2-350 °C	24.97036	101	0.0698	0.356311765	116.5717218	2.973E-13	7.359E-14	0.074295083
	37.7565	004	0.8315	0.238071505	10.09731838	3.433E-12	9.808E-12	0.885100918
	47.9617	200	1.48	0.189527733	5.87487404	5.900E-12	2.897E-11	1.575412597
	53.87141	105	0.92148	0.170047768	9.670307094	3.585E-12	1.069E-11	0.980889477
TiO_2-400 °C	24.98267	101	0.38254	0.356138983	21.2707162	1.629E-12	2.210E-12	0.407204862
	37.89613	004	0.14034	0.237226357	59.85055047	5.792E-13	2.792E-13	0.1493846
	47.99938	200	0.13555	0.189387746	64.15408345	5.403E-13	2.429E-13	0.144290397
	53.9502	105	0.19416	0.169818012	45.9111607	7.550E-13	4.744E-13	0.206679817

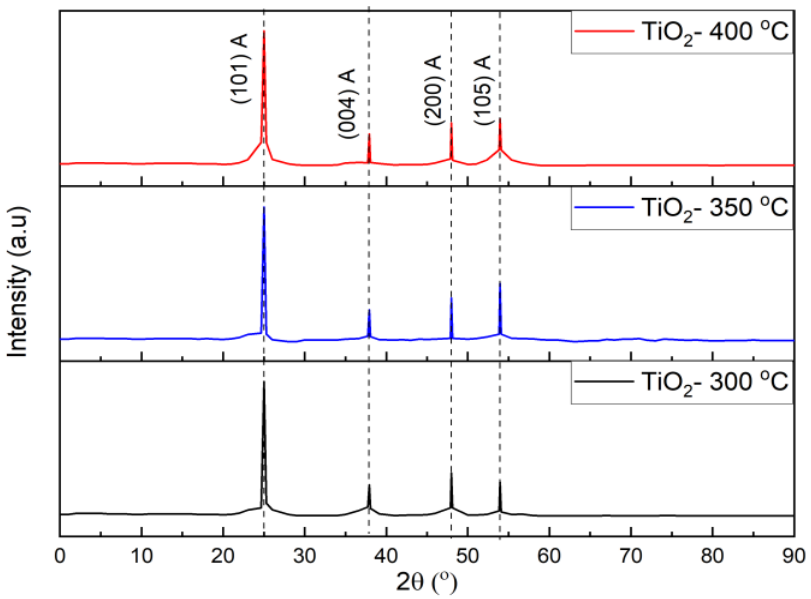

Figure 10 XRD spectra of TiO_2 thin films with 300, 350 and 400 °C.

3.4. Electrical properties

In order to investigate the effect of precursor concentration on the electrical properties of the TiO_2 thin films, we also calculated the electrical resistivity (ρ) and electrical conductivity (σ) of TiO_2thin films at ambient temperature using the following equations [41-45].

$$\rho = R_{sh} \times t \tag{10}$$

$$\sigma = \frac{1}{\rho} \tag{11}$$

$$F_{TC} = \frac{T}{R_{sh}} \tag{12}$$

whereR_{sh}, t, T, are the sheet resistance, thickness, and transmittance at 550 nm of the films, respectively [46-50]. Figure 12shows the variation of electrical conductivity and resistivity of thin films for different temperature. As can be seen, increasing the temperature up to 400ºC leads to electrical conductivity rise from 7.69×10^{-3} to 16.67×10^{-3} $(\Omega.cm)^{-1}$at temperature of 300 to 350 ºC, and then decreased to $9.0\times10^{-3}(\Omega.cm)^{-1}$at temperature of 400 ºC [51-54]. In contrast, the resistivity value decreases from 130 to 60(Ω.cm) and further increases to 110(Ω.cm) at temperature of 400 ºC temperature. The electrical parameters of the films are shown in Table 2. The figure of merit (F_{TC})of films decreases from 1.78×10^{-8} to $3.93\times10^{-8}(\Omega^{-1})$ at temperature of 300 to 350 ºC, and then decrease with the increasing of temperature to 400 ºC is $2.32\times10^{-8}(\Omega^{-1})$.

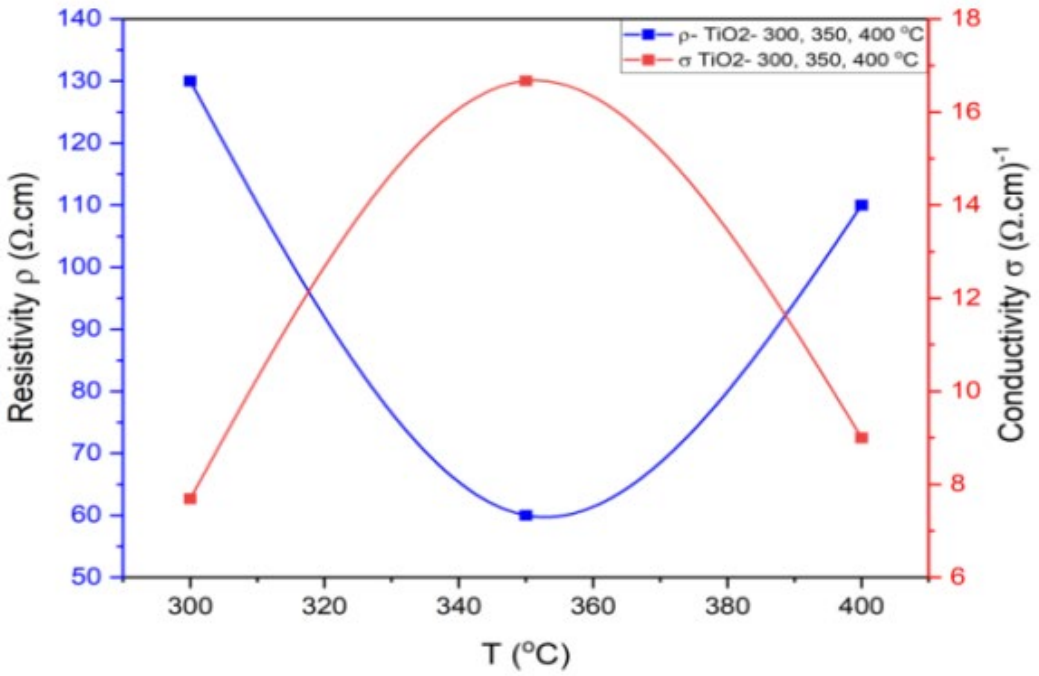

Figure 12 Electrical conductivity and resistivity variations of TiO_2 thin films with respect to the temperature.

Table 2 The electrical parameters of the TiO_2 films using Hall Effect with different temperatures 300, 350 and 400 ºC

Samples	Carrier Concentration n (cm^{-3})	Resistivity ρ (Ω cm)	Conductivity σ $(\Omega\ cm)^{-1} \times 10^{-3}$	Sheet resistance R_{sh} (Ω/sq) $\times 10^{+6}$	Mobility μ ($cm^2v^{-1}s^{-1}$)	Hall resistance RH (Ω)	Figure-of-merit F_{TC} $(\Omega^{-1}) \times 10^{-8}$
TiO_2-300 °C	0.5×10^{19}	130	7.69	5.63	0.0096	1.25	1.78
TiO_2-350 °C	1.46×10^{15}	60	16.67	2.88	71.347	4280.8	3.93
TiO_2-400 °C	3.21×10^{13}	110	9.0	5.59	1770.0	19470	2.32

The change in resistivity of TiO_2 thin films with increasing temperature can be influenced by various factors, and the specific behaviour may depend on the film's characteristics.

4. CONCLUSIONS

In this study, TiO_2 thin films were synthesized by dip-coating method. The effect of different temperature 300, 350 and 400 °C on the optical properties of TiO_2 thin films was investigated. A smaller bandgap may result in improved optical absorption in the visible and ultraviolet regions of the spectrum. The Urbach energy (E_u) value of TiO_2 films with various T has been deceased with the decreased of the bandgap (E_g) a material. The XRD patterns show that all the films are polycrystalline with a tetragonal anatase structure.

References

[1] I. Alshalal, H. M. I. Al-Zuhairi, A. A. Abtan, M. Rasheed, M. K. Asmail. J. Mech. Behav. Mater. 32 (2023) 1 https://doi.org/10.1515/jmbm-2022-0280
[2] M. Sellam, M. Rasheed, S. Azizi, T. Saidani. Ceram. Int. 50 (2024) 20917 https://doi.org/10.1016/j.ceramint.2024.03.094
[3] O. Alabdali, S. Shihab, M. Rasheed, T. Rashid. 3rd inter. Scient. conf. alkafeel univ. (ISCKU 2021) (2022) https://doi.org/10.1063/5.0066860
[4] M. Rasheed, O. Alabdali, S. Shihab, A. Rashid, T. Rashid, J. Phys.: Conf. Ser. 1999 (2021) 012078. https://doi.org/10.1088/1742-6596/1999/1/012078
[5] N. Assoudi et al. Opt. Quant. Electron. 54 (2022) 9 https://doi.org/10.1007/s11082-022-03927-x
[6] R. Jalal, S. Shihab, M.A. Alhadi, M. Rasheed, J. Phys.: Conf. Ser. 1660 (2020) 012090 https://doi.org/10.1088/1742-6596/1660/1/012090
[7] S. Shihab, M. Rasheed, O. Alabdali, A.A. Abdulrahman, J. Phys.: Conf. Ser. 1879 (2021) 022120. https://doi.org/10.1088/1742-6596/1879/2/022120
[8] A. Keziz, M. Heraiz, M. RASHEED, A. Oueslati. Mater Chem. Phys. 325 (2024) 129757 https://doi.org/10.1016/j.matchemphys.2024.129757
[9] D. Kherifi, A. Keziz, M. Rasheed, A. Oueslati. Ceram. Int. 50 (2024) 30175 https://doi.org/10.1016/j.ceramint.2024.05.317
[10] A. Jaber, M. Ismael, T. Rashid, M. A. Sarhan, M. Rasheed, I. M. Sala. Eureka: Phys. Eng. 4 (2023) 29 https://doi.org/10.21303/2461-4262.2023.002770
[11] T. Rashid, M. M. Mokji, M. Rasheed. J. Optics 47 (2024) 33 https://doi.org/10.1007/s12596-024-02080-w
[12] H. K. Aity, E. Dhahri, M. Rasheed. Ceram. Int. 50 (2024) 54666 https://doi.org/10.1016/j.ceramint.2024.10.324

[13] M. Rasheed, S. Shihab, O. Alabdali, A. Rashid, T. Rashid, J. Phys.: Conf. Ser. 1999 (2021) 012077 https://doi.org/10.1088/1742-6596/1999/1/012077
[14] M. Rasheed, M. Nuhad Al-Darraji, S. Shihab, A. Rashid, T. Rashid. J. Phys.: Conf. Ser. 1963 (2021) 012058 https://doi.org/10.1088/1742-6596/1963/1/012058
[15] A. Keziz, M. Heraiz, F. Sahnoune, M. Rasheed, Ceram. Int. 49 (2023) 32989 https://doi.org/10.1016/j.ceramint.2023.07.275
[16] E. Kadri, K. Dhahri, R. Barillé, M. Rasheed. Phase Transi. 94 (2021) 65 https://doi.org/10.1080/01411594.2020.1832224
[17] D. Bouras, M. Rasheed, Opt. Quantum Electron. 54 (2022) 12 https://doi.org/10.1007/s11082-022-04161-1
[18] A. Zubaidi, L.M. Asaad, I. Alshalal, M. Rasheed, J. Mech. Behav. Mater. 32 (2023) 1 https://doi.org/10.1515/jmbm-2022-0302
[19] M. Rasheed et al., J. Phys.: Conf. Ser. 1999 (2021) 012080 https://doi.org/10.1088/1742-6596/1999/1/012080
[20] M. Rasheed, M.N. Al-Darraji, S. Shihab, A. Rashid, T. Rashid, J. Phys.: Conf. Ser. 1963 (2021) 012059. https://doi.org/10.1088/1742-6596/1963/1/012059
[21] M. Enneffatia, M. Rasheed, B. Louati, K. Guidara, S. Shihab, R. Barillé, J. Phys.: Conf. Ser. 1795 (2021) 012050 https://doi.org/10.1088/1742-6596/1795/1/012050
[22] M. Rasheed, O.Y. Mohammed, S. Shihab, A. Al-Adili, J. Phys.: Conf. Ser. 1795 (2021) 012043 https://doi.org/10.1088/1742-6596/1795/1/012043
[23] A.H. Ali, A.S. Jaber, M.T. Yaseen, M. Rasheed, O. Bazighifan, T.A. Nofal, Complexity 2022 (2022) 1 https://doi.org/10.1155/2022/9367638
[24] M. Rasheed, et al., J. Adv. Biotechnol. Exp. Ther. 6) (2023) 495 https://doi.org/10.5455/jabet.2023.d144
[25] M. Rasheed, I. Alshalal, A.A. Ashed, M.A. Sarhan, A.S. Jaber, Indones. J. Electr. Eng. Comput. Sci. 33 (2024) 653 https://doi.org/10.11591/ijeecs.v33.i1.pp653-660
[26] I.M. Mohammed, M. Rasheed, AIP Conf. Proc. 3321 (2025) 020026 https://doi.org/10.1063/5.0289719
[27] F. Boudou, A. Belakredar, A. Berkane, M. Rasheed. Not. Sci. Biol. 17 (2025) 12183 https://doi.org/10.55779/nsb17212183
[28] F. Boudou, et al., Not. Sci. Biol. 17(3) (2025) 12593https://doi.org/10.55779/nsb17312593
[29] F. Boudou, A. Guendouzi, A. Belkredar. M. Rasheed, Not. Sci. Biol. 16 (2024) 13837 https://doi.org/10.55779/nsb16211837
[30] R.S. Mahmood et al. J. Mech. Behav. Mater. 34 (2025) 1 https://doi.org/10.1515/jmbm-2025-0040
[31] T. Rashid, M.M. Mokji, M. Rasheed, J. Mech. Behav. Mater. 34 (2025) 77 https://doi.org/10.1515/jmbm-2025-0074
[32] M. Rasheed, M. N. Mohammedali, F. A. Sadiq, M. A. Sarhan, T. Saidani. J. Optics (New Delhi. Print) (2024) https://doi.org/10.1007/s12596-024-01928-5
[33] A.J. Hussein, M.N. Al-Darraji, M. Rasheed, M.A. Sarhan, IOP Conf. Ser.: Earth Environ. Sci. 1262 (2023) 022007 https://doi.org/ 10.1088/1755-1315/1262/2/022007
[34] A.J. Hussein, M.N. Al-Darraji, M. Rasheed, M.A. Sarhan, IOP Conf. Ser.: Earth Environ. Sci. 1262 (2023) 022005 https://doi.org/10.1088/1755-1315/1262/2/022005
[35] T. Saidani, M. Rasheed, I. Alshalal, A.A. Rashed, M.A. Sarhan, R. Barillé, Res. Eng. Struct. Mater. 10 (2024) 743 http://dx.doi.org/10.17515/resm2023.21ma0922rs
[36] M. A. Sarhan, S. Shihab, B. E. Kashem, M. Rasheed, J. Phy.: Conf. Ser., 1879 (2021) 022122 https://doi.org/10.1088/1742-6596/1879/2/022122
[37] M. Rasheed, O. Alabdali, S. Shihab, J. Phy.: Conf. Ser. 1879 (2021) 032120 https://doi.org/10.1088/1742-6596/1879/3/032120
[38] M. Rasheed, R. Barillé, J. Non-Cryst. Solids., 476 (2017) 1 https://doi.org/10.1016/j.jnoncrysol.2017.04.027

[39] M. Rasheed, R. Barillé, Opt. Quantum Electron. 49 (2017) 33 https://doi.org/10.1007/s11082-017-1030-7
[40] F. Dkhilalli, S. M. Borchani, M. Rasheed, R. Barille, K. Guidara, M. Megdiche, J. Mater. Sci. Mater. Electron, 29 (2018) 6297 https://doi.org/10.1007/s10854-018-8609-z.
[41] A. Boumezoued, K. Guergouri, Régis Barillé, Rechem Djamil, Mourad Zaabat, M. Rasheed, J. Alloys Compd. 791 (2019) 550 https://doi.org/10.1016/j.jallcom.2019.03.251
[42] N. Ben Azaza et al., Opt. Mater., 96 (2019) 109328 https://doi.org/10.1016/j.optmat.2019.109328
[43] Areej Adnan Hateef, Essebti Dhahri, M. Rasheed, Habiba Kadhim, Z. Abbas, N. Hassan, Study of the influence concentration difference of copper in properties of cerium nanopowder, Physics and Chemistry of Solid State, 25 (2024) 801 https://doi.org/10.15330/pcss.25.4.801-810
[44] M. Rasheed, SuhaShihab, O. Alabdali, H. H. Hassan, J. Phys. Conf. Ser., 1879 (2021) 032113 https://doi.org/10.1088/1742-6596/1879/3/032113
[45] H. K. Aity, M. Rasheed, E. Dhahri, A. A. Hateef, T. Saidani, Chromium-doped magnesium oxide nanoparticles: dielectric insights and antibacterial potentials, Journal of Materials Science, 61 (2026) 6226 https://doi.org/10.1007/s10853-026-12241-w
[46] T. Saidani, S. Mokhtari, M. Rasheed, H. Lahmar, M. Trari, Annealing temperature dependent properties ZnO–TiO_2 bilayer thin films: characteristics and photocatalytic activity, Journal of the Indian Chemical Society, 103 (2026) 102499 https://doi.org/10.1016/j.jics.2026.102499
[47] M. RASHEED, A. Khaleefah, Materials Chemistry and Physics, 353 (2026) 132112 https://doi.org/10.1016/j.matchemphys.2026.132112
[48] S. S. Batros, M. Rasheed, H. K. Aity, A. A. Hatef, T. Saidani, Materials Chemistry and Physics, 355 (2026) 132243 https://doi.org/10.1016/j.matchemphys.2026.132243
[49] A. Raghdi, M. Heraiz, M. Rasheed, A. Keziz, Investigation of halloysite thermal decomposition through differential thermal analysis (DTA): Mechanism and kinetics assessment, Journal of the Indian Chemical Society, 101 (2024) 101413 https://doi.org/10.1016/j.jics.2024.101413.
[50] A. I. A. Ali, M. RASHEED, Effect of changing magnetite percentage on structural and magnetic properties of cobalt ferrite prepared by the sol-gel method, Experimental and Theoretical NANOTECHNOLOGY 10 (2026) 277 https://doi.org/10.56053/10.s.277
[51] A. Khaleefah, M. RASHEED, Sol–gel-derived mullite nanoparticles: Structural and antibacterial insights, Experimental and Theoretical NANOTECHNOLOGY 10 (2026) 289 https://doi.org/10.56053/10.s.289
[52] Z. S. Ahmed, M. RASHEED, H. S. Ahmed, Optimizing NiO nanoparticle properties for antibacterial applications via temperature-driven structural modification, Experimental and Theoretical NANOTECHNOLOGY 10 (2026) 329 https://doi.org/10.56053/10.s.329
[53] Z. S. Ahmed, M. RASHEED, H. S. Ahmed, Enhancing α-Bi_2O_3 nanoparticle crystallinity and antibacterial functionality through controlled calcination, Experimental and Theoretical NANOTECHNOLOGY 10 (2026) 343 https://doi.org/10.56053/10.s.343
[54] A. I. A. Ali, M. RASHEED, Effect of sintering temperature on electrical and structural properties for spinel ferrites prepared by sol-gel method, Experimental and Theoretical NANOTECHNOLOGY, 10 (2026) 239 https://doi.org/10.56053/10.s.239

Exp. Theo. NANOTECHNOLOGY 10 (2026) 795-809